University Turbine Systems Research (UTSR)

Industrial Fellowship Program

2014

Final Report

Validation of a combustion oscillation model against experimental results

Prepared For:

Solar Turbines, Inc.

Mentor: James Blust

2200 Pacific Highway

San Diego, CA 92186

&

Southwest Research Institute (SWRI)

Mechanical Engineering Division

6220 Culebra Road

San Antonio, TX 78238

Prepared By:

Bridget O'Meara

PhD candidate, Mechanical Engineering

Pennsylvania State University

University Park, PA 16801

1 Introduction

Gas turbines must operate under lean, pre-mixed conditions in order to meet current nitrogen oxide (NOx) emissions regulations. However, lean, pre-mixed combustors are susceptible to combustion instabilities that can cause problems including including lower efficiency, flame blowout and flashback, and vibrations that may damage or destroy the system components. Instabilities occur due to coupling between oscillations in combustor pressure, inlet velocity and equivalence ratio, and the flame's heat release.

This coupling is illustrated by the feedback loop in Figure 1. When heat release oscillations occur in phase with pressure oscillations, energy is added to the acoustic disturbance. Pressure oscillations then perturb the mass flow rates of air and fuel. Variations in air flow rate lead to inlet velocity oscillations, while both air and fuel flow rate variations cause equivalence ratio oscillations. Many studies focus on fully pre-mixed flames in which well mixed air and fuel enter the system, preventing equivalence ratio oscillations. This simplification makes fully pre-mixed flames easier to study, but actual gas turbines are run technically pre-mixed in which fuel is injected further downstream and both velocity and equivalence ratio oscillations are present. Heat release oscillations are then comprised of a component due to inlet velocity oscillations and a component due to equivalence ratio oscillations. The total heat release depends on the magnitude and phase of both components.

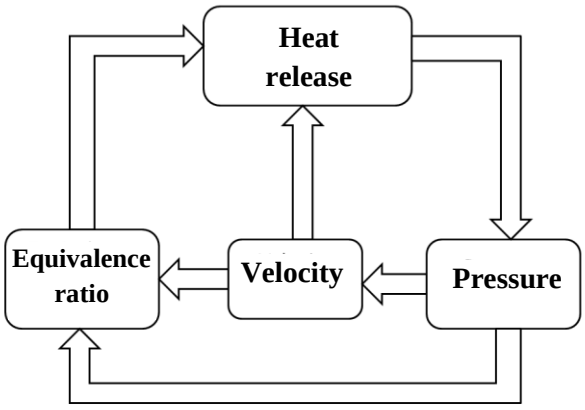

Figure 1: Combustion oscillation feedback loop

An accurate model of the combustion system is necessary to predict the stability characteristics of a combustor and prevent oscillations from occurring. Simple acoustic models can predict the natural frequencies of the system, but in order to accurately predict self-excited instabilities, a model must include the heat release oscillations that drive the instability. This report details a study of the heat release feature of an acoustic network model and includes validation against experimental results. The model's sensitivity to flame temperature, and to the gain and phase of

the velocity and equivalence ratio heat release components was tested. The effect of an inlet area restriction was also tested.

2 PSU test rig design and model

2.1 Test rig design

Experimental results were obtained prior to the period of this internship using a test facility at Pennsylvania State University (PSU) as part of the author's thesis research. Figure 2 illustrates the PSU test rig which includes a Solar Turbines Taurus 70 injector. The flow direction in the schematic is from left to right with air entering through the section labeled (a). Fuel is added in the injector and the air and fuel mix over the distance between the fuel injection location and the combustor. The combustor is made up of two sections. A quartz window section allows optical access to the flame. The combustor length can be varied by adjusting the axial location of a plug located inside the stainless steel downstream section. The variable length combustor allows the acoustics of the system to be tuned to excite or damp instabilities.

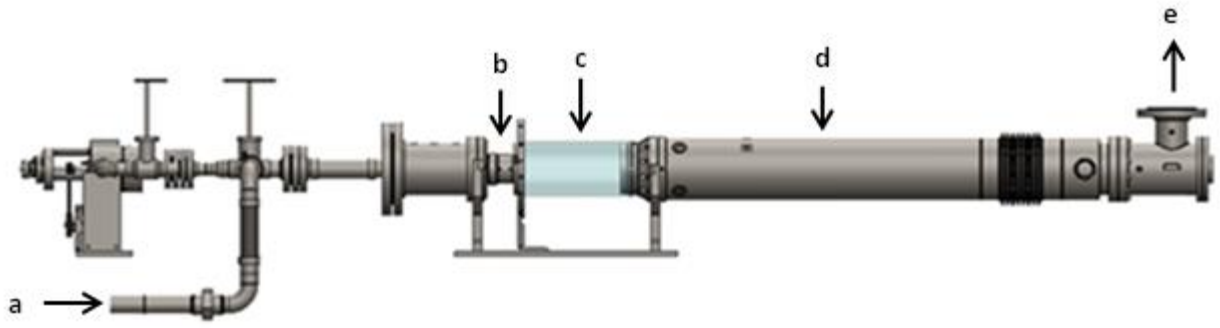

Figure 2: PSU test rig schematic: a) Inlet air – Flow direction is from left to right; b) Solar Turbines Taurus 70 injector; c) Quartz combustor section -- Quartz window allows optical access to the flame; d) Stainless steel combustor section – The axial location of a plug inside this section can be varied

Figure 3 shows a schematic of the Taurus 70 injector in the PSU rig. The injector includes a plate that creates an area restriction upstream of the swirler. The effect of the location of this area restriction on combustor's stability was tested experimentally. Experimental results were obtained with the restriction in its baseline location as well as 1in. and 2in. upstream of the baseline location. These locations are indicated in Figure 3 by a blue, red, and green line, respectively. The effects of the area restriction location will be discussed in Section 3.3.

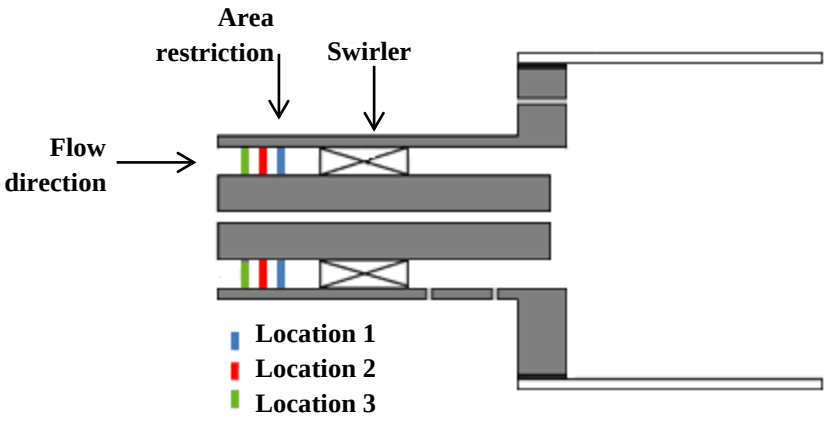

Figure 3: Schematic of the Taurus 70 injector in the PSU rig. Colored lines indicate the location of the inlet area restriction

2.2 Acoustic network model

The model used in this study is a one-dimensional acoustic network model. In this model, the somewhat complicated geometry of the PSU test rig is broken down into a series of ducts of uniform geometry, flow rate, and temperature. Figure 4a shows a schematic of the geometry used in the model. These sections are connected at junctions where boundary conditions are defined. The network of ducts and junctions are shown in Figure 4b. Boundary conditions include pressure and volume matching conditions at changes in duct area, flow rate, or temperature, impedance conditions for swirlers and area restrictions, heat release at the flame, and open or closed end conditions.

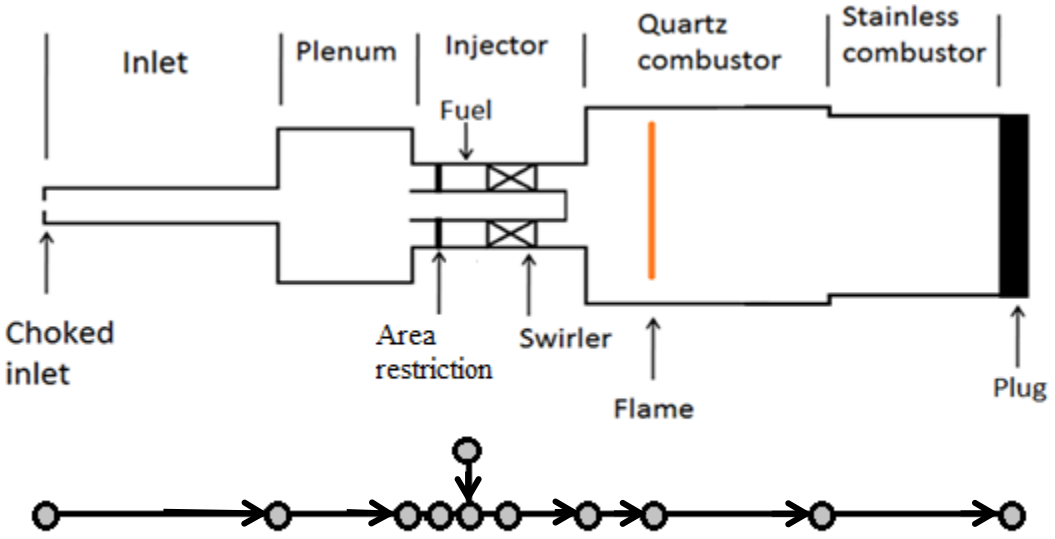

Figure 4: a) Simplified geometry of the PSU test rig used in the acoustic network model; b) Connections of ducts – straight lines indicate ducts, arrows indicate flow direction, and circles indicate nodes where ducts are connected and boundary conditions are defined

3 Validation of acoustic network model

3.1 Effect of equivalence ratio

The plots in Figure 5 show normalized combustor pressure oscillations plotted against combustor length. These results were obtained experimentally in the PSU test rig. The combustor length, L_{comb}, was varied from 25 in. to 59 in. at 1in. increments by varying the axial location of a plug located in the downstream, stainless steel section of the combustor. Different combustor lengths excite instabilities of different magnitudes and frequencies. Peaks in pressure oscillations indicate unstable combustor lengths. The frequencies of two instabilities which will be studied in further detail are also indicated in the figure.

The case shown in Figure 5a has a lower equivalence ratio (φ) than the case shown in Figure 5b. Varying the equivalence ratio changes the stability characteristics of the combustor. In the lower equivalence ratio case (ϕ = 0.55), there is a large instability for 39 in. < L_{comb} < 45 in. This corresponds to a frequency of about 360 Hz. When the equivalence ratio is increased to ϕ = 0.60, the 360 Hz instability is damped. However, an instability is excited for 30 in. < L_{comb} < 34 in. with a frequency of about 450 Hz. This instability was not observed in the lower equivalence ratio case.

a)

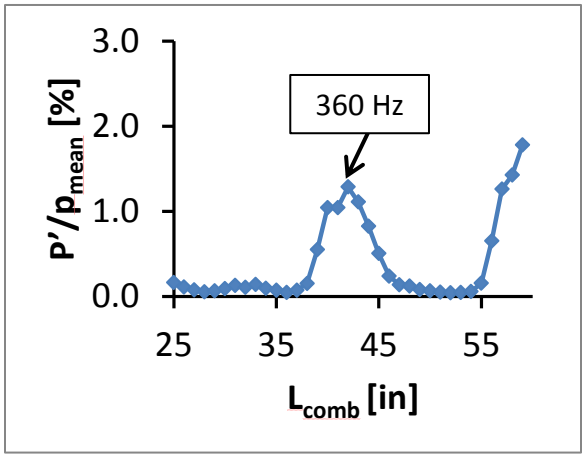

b)

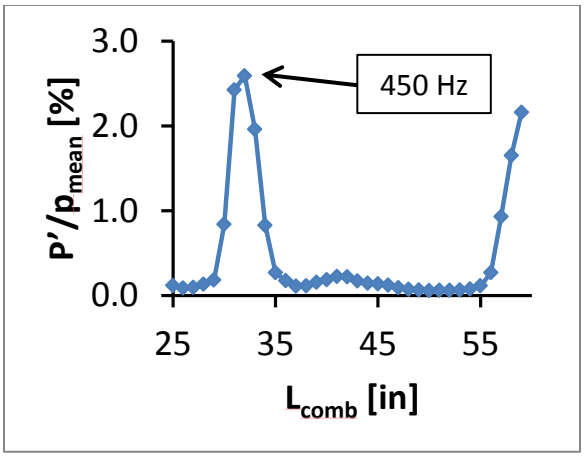

Figure 5: PSU rig stability maps with instability frequency indicated
a) Tin = 250°C, uin = 40 m/s, ϕ= 0.55
b) Tin = 250°C, uin = 40 m/s, ϕ= 0.60

The acoustic network model was tested to capture the equivalence ratio effect observed in experiments. Increasing the equivalence ratio increases the flame temperature. Therefore, for a combustor length of 41in., the model should predict a 360 Hz instability at low flame temperatures but not at high flame temperatures. Similarly, for a combustor length of 32in., the model should predict a 450 Hz instability at higher flame temperatures but not at lower flame temperatures.

As mentioned in Section 1, heat release oscillations are caused by both velocity and equivalence ratio oscillations. Both the velocity and equivalence ratio components can be described by a gain and phase value. The gain indicates whether the disturbance amplifies or damps heat release oscillations, and the phase indicates the time delay between the disturbance and the heat release oscillation. The user inputs these values into the model. Unfortunately, these values have not yet been obtained experimentally, so in this study, these parameters were adjusted to values where model results matched experimental results.

The acoustic model gives results in terms of an instability frequency and growth rate. Negative growth rates indicate the instability will be damped and positive growth rates indicate the instability will grow. If multiple positive growth rates are predicted, the frequency with the largest positive growth rate will dominate. Figure 6 shows the frequencies and growth rates predicted by the model at various flame temperatures with the combustor length set to 41 in. The adiabatic flame temperature is approximately 1800K when $\phi = 0.55$ and approximately 1900K when $\phi = 0.60$. However, due to heat transfer, the actual combustor temperature is expected to be as much as 100K lower than the adiabatic flame temperature. The model then predicts an instability of approximately 360 Hz with a positive growth rate in the range of temperatures possible for $\phi = 0.55$ while the growth rate is negative in the range of temperatures possible for with $\phi = 0.60$. These results are consistent with experimental results.

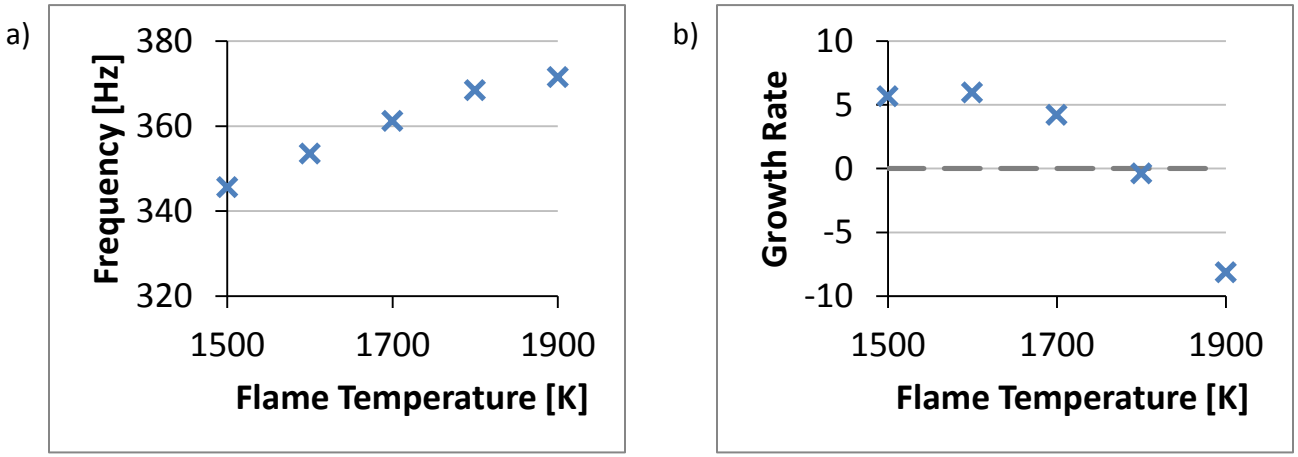

Figure 6: a) Frequency and b) Growth Rate predictions for L_{comb} = 41in
$Gain_u$ = 0.25; $Phase_u$ = 0; $Gain_\phi$ = 1; $Phase_\phi$ = 225

Similarly, the model predicts an instability of approximately 450 Hz with a positive growth rate in the range of temperatures possible for with $\phi = 0.60$ while the growth rate is negative in the range of temperatures possible for with $\phi = 0.55$. These results are also consistent with experimental results.

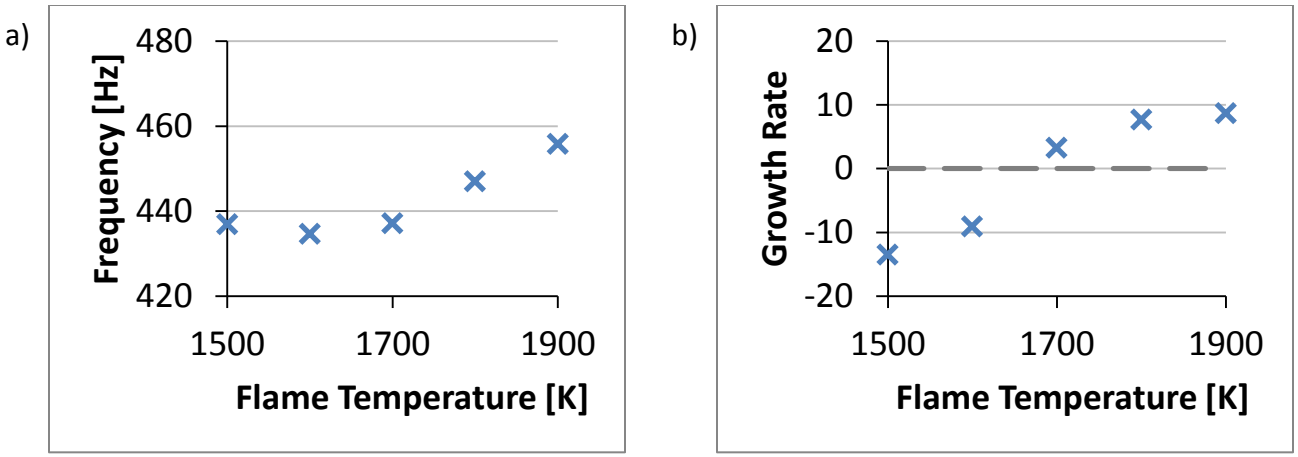

Figure 7: a) Frequency and b) Growth Rate predictions for Lcomb = 32in
$Gain_u$ = 0. 5; $Phase_u$ = 0; $Gain_\phi$ = 1; $Phase_\phi$ = 0

3.2 Sensitivity to heat release gain and phase

It is worth noting the sensitivity of the model to the gain and phase of the velocity and equivalence ratio heat release components. The gain values chosen for the L_{comb} = 41in. case indicate that the equivalence ratio component is dominant (larger gain value), and the phase values indicate the two components are out of phase. Gain and phase values are frequency dependent, so the values are expected to change between the L_{comb} = 41in case (360 Hz) and L_{comb} = 32in. case (450 Hz). The selected values still show a dominant equivalence ratio component, but in this case the two components are in phase.

The results predicted by the model are strongly dependent on the selected values of gain and phase. For example, Figures Figure 8 and Figure 9 show the model results do not match experimental results when using the program's default gain and phase values of one and zero, respectively, for both the velocity and equivalence ratio components. In both the L_{comb} = 41in. and L_{comb} = 32in. cases, the model predicts frequencies that are lower than experimental results and positive growth rates for over the entire temperature range tested.

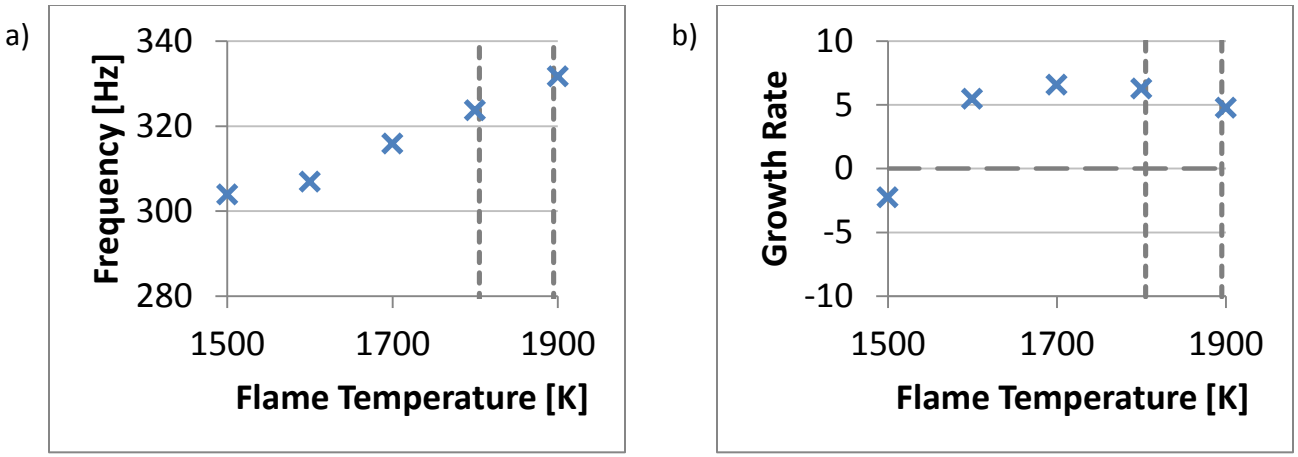

Figure 8: a) Frequency and b) Growth Rate predictions for Lcomb = 41in
$Gain_u$ = 1; $Phase_u$ = 0; $Gain_\phi$ = 1; $Phase_\phi$ = 0

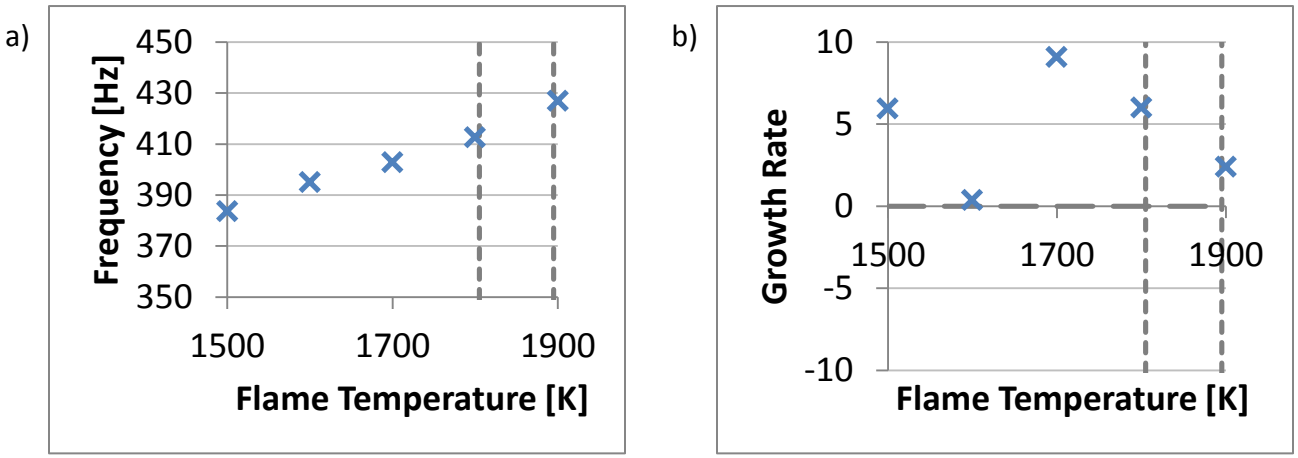

Figure 9: a) Frequency and b) Growth Rate predictions for Lcomb = 32in
$Gain_u$ = 1; $Phase_u$ = 0; $Gain_\phi$ = 1; $Phase_\phi$ = 0

3.3 Effect of area restriction location

Figure 10 compares the stability of the PSU rig with the area restriction plate in three locations. Figure 10a shows a reduction in the 39 in. < L_{comb} < 45 in. instability when the restriction is moved upstream. However, Figure 10b shows that moving the plate upstream makes the 30 in. < L_{comb} < 34in. instability worse. The mechanism responsible for the effect of the area restriction location cannot be determined directly from available experimental results, but the results do suggest the effect depends on the frequency of the instability.

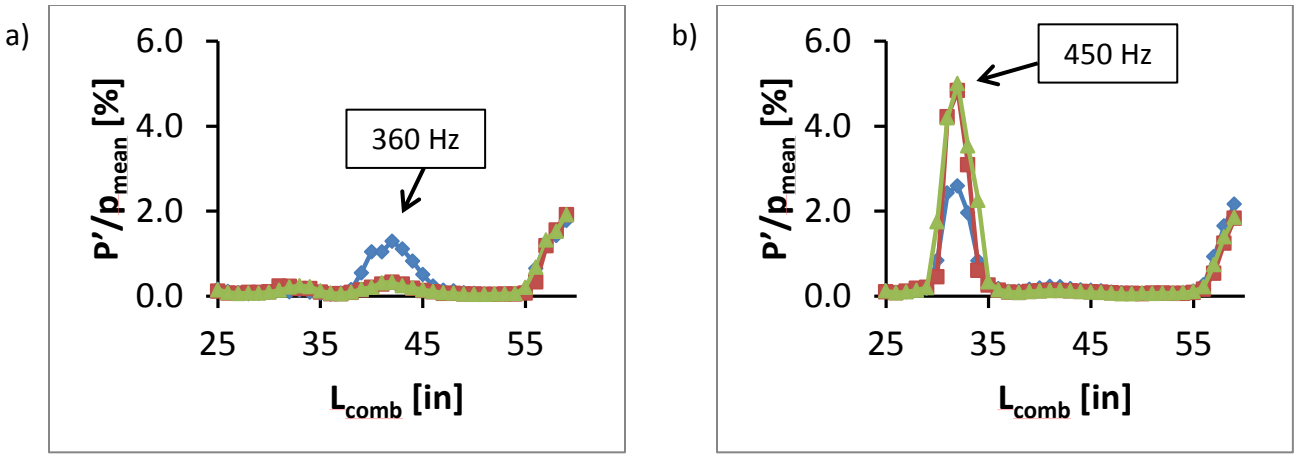

Figure 10: Stability maps showing the effect of area restriction location: baseline location (blue), 1in. upstream (red), and 2in. upstream (green)
a) Tin = 250°C, uin = 40 m/s, ϕ= 0.55
b) Tin = 250°C, uin = 40 m/s, ϕ= 0.60

The location of the plate was varied in the model geometry. Figure 11 shows the frequencies and growth rates predicted by the model for various flame temperatures for the Lcomb = 41in. case. Blue x's indicate the plate in the original location and green x's indicate the 2in. upstream location. The model shows no change in results when the area restriction location varied. The plate location does not affect acoustic response of the system, indicating the plate effect is not a purely acoustic effect. Another mechanism must be responsible for the effects observed in experiments.

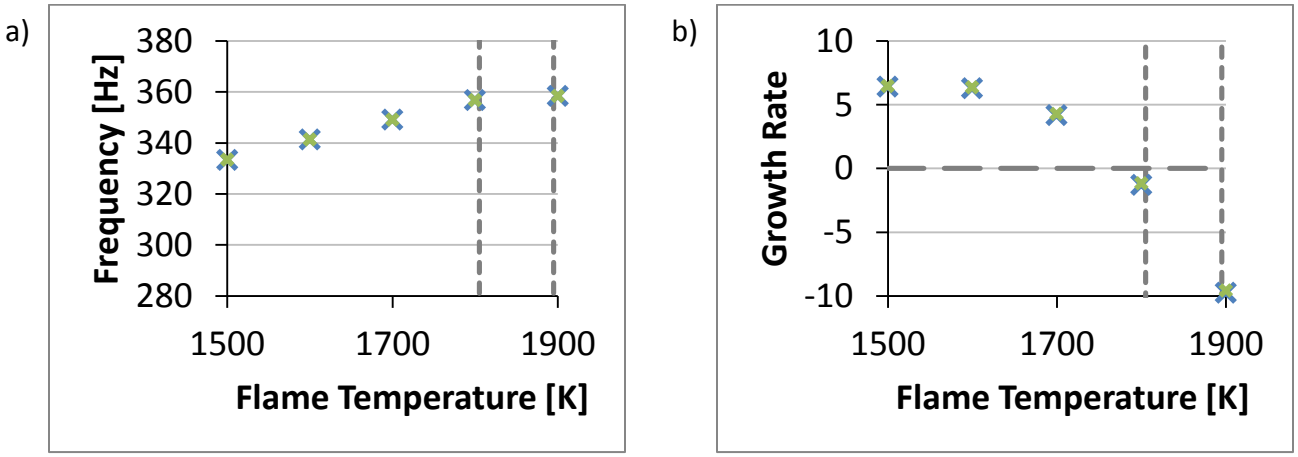

Figure 11: Predicted frequencies and growth rates with the area restriction in the original location (blue) and 2in. upstream (green)

It was hypothesized that the area restriction may act as a boundary that creates change in the phase air flow rate oscillations. Considering the sensitivity of the model to the gain and phase values of the heat release components, a change in phase is likely to have a strong effect on the

model predictions. Figure 12 shows the effect of changing the phase of the velocity component of heat release. Increasing the phase decreases the predicted growth rate while the frequency remains approximately the same. If the phase is increased past 40°, the growth rates for all flame temperatures tested fall into the negative range, indicating the 360 Hz instability will be damped. This explains why experiments showed the restriction location reduced the amplitude of the instability while the frequency of the instability remained approximately unchanged.

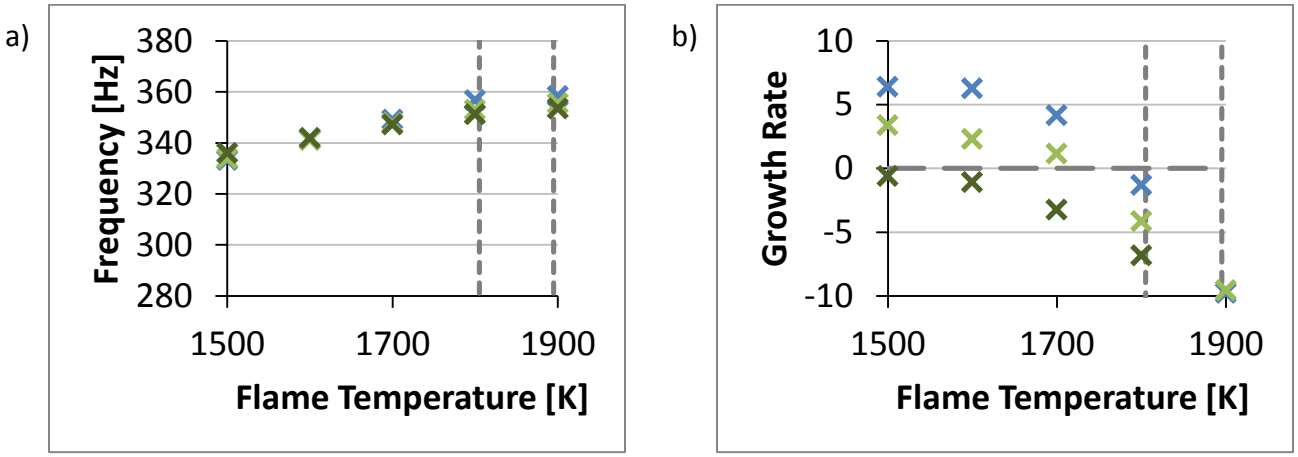

Figure 12: Effect of velocity component phase on model results. The blue, light green, and dark green x's indicate phase values of 0°, 20°, and 40° respectively

4 Application of acoustic model to Solar Taurus 70 engine oscillations

Validation of the acoustic network model is important to Solar Turbines because this model is useful in developing engine designs. This section provides an example of how the model can be applied to an actual engine. Previous work performed at Solar Turbines showed that the Taurus 70 engine experiences a 200 Hz instability when operated at partial load. Acoustic modeling of this engine also showed a 200 Hz natural frequency at this operating condition. A Helmholtz resonator design was proposed to reduce these instabilities. Size constraints within the engine determined the size and location of the resonators. As part of this internship, the Helmholtz resonators were added to the acoustic model of the Taurus 70.

Figure 13 shows the natural frequency mode shapes for the Taurus 70 engine without (Figure 13 a) and with (Figure 13 b) the Helmholtz resonators. The plots show the normalized pressure amplitude versus the axial location along the engine. The model cannot predict the exact amplitude of the oscillations, but the change in the mode shape with the addition of Helmholtz resonators indicates that the resonators will affect the instability. Although further optimization

of the design and experimental testing are still necessary, the change in mode shapes gives confidence in proceeding with this resonator design.

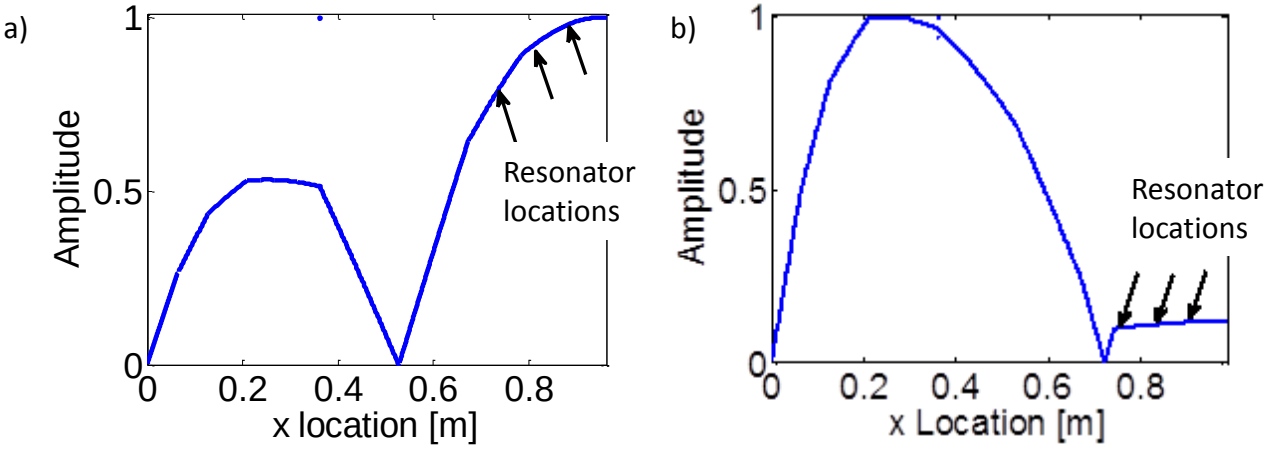

Figure 13: 200 Hz natural frequency mode shapes for the Taurus 70 engine a) without Helmholtz resonators; b) with Helmholtz resonators

5 Conclusions and Future Work

An acoustic network model with heat release was validated against experimental data. The model captured the effect of equivalence ratio observed in experiments, but showed strong sensitivity to the gain and phase of the velocity and equivalence ratio components of heat release. The model also showed that the effect of the location of an area restriction in the injector is likely due to a change in the phase of the air flow rate oscillations, rather than a purely acoustic effect. The acoustic model was also used to test a Helmholtz resonator design for the Taurus 70 engine. The model demonstrated that a Helmholtz resonator can affect the 200 Hz instability.

The sensitivity of the model to the heat release velocity and equivalence ratio component requires further study in the future to better understand this relationship. Experimental measurements of the gain and phase are necessary. The model should also be systematically tested through a wide range of gain and phase values to fully understand the effect of these parameters. Future work on the resonator design will involve optimizing the design and experimental testing.

6 Acknowledgements

I would like to thank Southwest Research Institute (SWRI), the University Turbine Systems Research (UTSR) program, and Solar Turbines, Inc. for providing me with this opportunity. I would also like to all those at Solar Turbines who helped and supported me throughout my internship. I have learned so much about gas turbines and the gas turbine industry through this experience, and I am certain that the knowledge I've gained throughout this program will help me as I continue with my graduate research.